The Astrophysical Journal, 637:104–113, 2006 January 20

TYPE I ULTRALUMINOUS INFRARED GALAXIES: TRANSITION STAGE FROM ULIRGs TO QSOs

Nozomu Kawakatu
International School for Advanced Studies, Via Beirut 2-4, 34014 Trieste, Italy; kawakatu@sissa.it

Naohisa Anabuki
Department of Earth and Space Science, Graduate School of Science, Osaka University, 1-1 Machikaneyama, Toyonaka, 560-0043 Osaka, Japan; anabuki@ess.sci.osaka-u.ac.jp

Tohru Nagao
Osservatorio Astrofisico di Arcetri, Largo Enrico Fermi, 5, 50125 Firenze, Italy; and National Astronomical Observatory of Japan, 2-21-1 Osawa, Mitaka, Tokyo 151-8588, Japan; tohru@arcetri.astro.it

Masayuki Umemura
Center for Computational Sciences, University of Tsukuba, Ten-nodai, 1-1-1 Tsukuba, Ibaraki 305-8577, Japan; umemura@ccs.tsukuba.ac.jp

and

Takao Nakagawa
Institute of Space and Astronautical Science, Japan Aerospace Exploration Agency, 3-1-1 Yoshinodai, Sagamihara, Kanagawa 229-8510, Japan; nakagawa@ir.isas.jaxa.jp
Received 2005 June 21; accepted 2005 September 14

ABSTRACT

We examine whether the ultraluminous infrared galaxies that contain a type 1 Seyfert nucleus (a type I ULIRG) are in the transition stage from ULIRGs to quasi-stellar objects (QSOs). To investigate this issue, we compare the black hole (BH) mass, the bulge luminosity, and the far-infrared luminosity among type I ULIRGs, QSOs, and elliptical galaxies. As a result, we find the following results: (1) The type I ULIRGs have systematically smaller BH masses in spite of the comparable bulge luminosity relative to QSOs and elliptical galaxies. (2) The far-infrared luminosity of most type I ULIRGs is larger than the Eddington luminosity. We show that the above results do not change significantly for three type I ULIRGs for which we can estimate the visual extinction from the column density. Also, for all eight type I ULIRGs, we investigate the effect of uncertainties of BH mass measurements and our sample bias to make sure that our results are not altered even if we consider the above two effects. In addition, Anabuki recently revealed that their X-ray properties are similar to those of the narrow-line Seyfert 1 galaxies. These would indicate that active galactic nuclei (AGNs) with a high mass accretion rate exist in type I ULIRGs. On the basis of all of these findings, we conclude that it would be a natural interpretation that type I ULIRGs are the early phase of BH growth, namely, the missing link between ULIRGs and QSOs. Moreover, by comparing our results with a theoretical model of a coevolution scenario of a QSO BH and a galactic bulge, we show clearly that this explanation could be valid.

Subject headings: black hole physics — galaxies: active — galaxies: bulges — galaxies: formation — galaxies: starburst — quasars: general

Online material: color figures

1. INTRODUCTION

Recently, the *Infrared Astronomical Satellite* (*IRAS*) made the remarkable discovery of a new class of galaxies, the ultraluminous infrared galaxies [ULIRGs, i.e., those having infrared luminosities greater than $L_{\rm IR}(8-1000\ \mu{\rm m}) \geq 10^{12}\ L_{\odot}$], which emit the bulk of their energy at infrared wavelengths. Several studies (e.g., Sanders & Mirabel 1996) have established that ULIRGs are gas-rich galaxies that in most cases have undergone a recent strong interaction with other galaxies eventually leading to a complete merger of the two. A commonly accepted explanation is that during such a galaxy collision the interstellar medium is transported toward the circumnuclear environment and is concentrated and compressed there, thus resulting in starburst on scales of less than a few kiloparsecs. In the next phase, the low angular momentum gas in the starburst region may fall into and accrete onto the central massive BH. In addition, the luminosity and space density of ULIRGs are similar to those of QSOs. Moreover, the luminosity function of *IRAS* galaxies is of a double power-law type and thus differs from that of the normal galaxies that show exponential rollover and is rather similar to that of QSOs or starbursts (Scoville 1992). Thus, it has been suggested that ULIRGs are powered by heavily obscured QSOs (e.g., Sanders et al. 1988) or starbursts (Joseph & Wright 1985). However, the physical relation between ULIRGs and QSOs has been an issue of long standing.

For early-type galaxies and QSOs, recent high spatial resolution observations have suggested that the mass of a supermassive black hole (SMBH) tightly correlates with the mass, the velocity dispersion, and the luminosity of the galactic bulge (e.g., Kormendy & Richstone 1995; Richstone et al. 1998; Laor 1998; Tremaine et al. 2002; McLure & Dunlop 2001, 2002; Marconi & Hunt 2003; Kawakatu & Umemura 2004). It has been found that the relatively low z QSO hosts are mostly luminous and well-evolved early-type galaxies (e.g., McLeod & Rieke 1995; Bahcall et al. 1997; Hooper et al. 1997; McLeod et al. 1999; Brotherton et al. 1999; Kirhakos et al. 1999; McLure et al. 1999, 2000; Falomo et al. 2004; Dunlop et al. 2003). Recently, Veilleux

et al. (1999) have shown that the percentage of AGNs is 30%–50% for $L_{\rm IR} > 10^{12}\ L_{\odot}$. These findings suggest that the formation of ULIRGs, SMBHs, galactic bulges, and QSOs could be related to each other. However, this physical link is an open question.

From the theoretical point of view, Kawakatu et al. (2003; hereafter KUM03) suggested a potential mechanism for building up an SMBH. They consider the effect of radiation drag,[1] which extracts angular momentum from the interstellar medium in starburst galaxies and thereby drives the mass accretion onto the galactic center (Umemura 2001; Kawakatu & Umemura 2002; Sato et al. 2004). On the basis of the radiation drag model, they proposed a new picture for QSO formation. First, they regarded classical ULIRGs as starburst galaxies, in which there is little AGN activity (if any). Next, they predicted the possibility of the "proto-QSO phase." In this phase, the galaxies are optically thin and the total luminosity is still dominated by bulge stars, although there is significant AGN activity in them. In this phase, a BH is still growing through mass accretion and the BH-to-bulge mass ratio is smaller than that of QSOs and elliptical galaxies. Then once the BH is fully grown and the central AGN dominates the total luminosity, the galaxy is regarded as a QSO (see also figures in KUM03). However, no proto-QSO has yet been identified observationally, although it is essential to clarify which objects correspond to proto-QSOs.

Recently, ultradeep X-ray observations have suggested that submillimeter galaxies (SMGs) at $z \simeq 1-3$ have mass accretion rates $\sim$1 order of magnitude lower than those of coeval QSOs, assuming Eddington luminosity (Alexander et al. 2005). Moreover, Borys et al. (2005) found that SMGs have smaller BH masses than QSOs with respect to the same mass range of bulges, and thus the SMGs may correspond to the "proto-QSO" predicted in KUM03. In nearby galaxies, Canalizo & Stockton (2001) proposed that infrared-selected type I AGNs (hereafter type I ULIRGs) are a transitional stage between ULIRGs and QSOs as their host galaxies are undergoing tidal interactions or mergers accompanied by massive starbursts (see also Zheng et al. 2002; Lípari et al. 2005). In addition, most of them show an FWHM of the broad Hβ line of less than 2000 km s^{-1} (Zheng et al. 2002); thus, AGNs would actually be narrow-line Seyfert 1 galaxies (NLS1's). Recently, Anabuki (2004) studied 27 ULIRGs using X-ray imaging and spectroscopic observations with *ASCA* (*Advanced Satellite for Cosmology and Astrophysics*), *Chandra*, and *XMM-Newton*. Among their sample, 10 ULIRGs were identified as type I ULIRGs. After correcting the absorption effects, he found that seven luminous type I ULIRGs show a soft X-ray excess, a spectral energy distribution with a steep photon index ($\Gamma_{2-10\,\rm kev} > 2$), and also a violent flux change (excess variance $\sim$0.01–0.1), which are characteristic properties of NLS1's. These X-ray properties imply that AGNs with smaller BHs and high mass accretion rates exist in type I ULIRGs (e.g., Pounds et al. 1995; Boller et al. 1996; Mineshige et al. 2000). Moreover, Mathur (2000) suggested that NLS1's may be Seyfert 1 galaxies in the early stage of their evolution if the BHs in NLS1's are undermassive with respect to their host bulges. Hence, it is likely that all of the above characteristics support the hypothesis that type I ULIRGs are the early phase of BH growth. However, the previous works have never examined the BH-to-bulge relation among type I ULIRGs, QSOs, and elliptical galaxies. By investigating this issue, we can reveal whether type I ULIRGs have systematically smaller BHs than QSOs and elliptical galaxies. By combining the BH-bulge relation for type I ULIRGs with the previous works for type I ULIRGs, we test whether they are really proto-QSOs, which are the transition phase from ULIRGs into QSOs. To this end, we demonstrate the relation among type I ULIRGs, QSOs, and elliptical galaxies of the BH mass ($M_{\rm BH}$) versus the absolute R-band magnitude of the galactic bulge [M_R(bulge)]. In addition, we examine the BH mass ($M_{\rm BH}$) and far-infrared (FIR) luminosity ($L_{\rm FIR}$) for type I ULIRGs and QSOs in order to constrain the origin of type I ULIRGs.

The paper is organized as follows. In § 2, we describe how type I ULIRGs, QSOs, and elliptical galaxies are selected. In § 3, we briefly review the technique of estimating BH masses from the broad emission-line widths for type I ULIRGs. In § 4, we plot the data of type I ULIRGs in the $M_{\rm BH}$-M_R(bulge) diagram and also compare them with those of QSOs and elliptical galaxies. Next, we show the $M_{\rm BH}$-$L_{\rm FIR}$ relation for type I ULIRGs and QSOs and then compare with each other. Finally, we constrain the optical extinction of the central regions for type I ULIRGs by using the results of hard X-ray observations. In § 5, we summarize our observational results for the type I ULIRGs, and then we compare them with one of the theoretical models (KUM03 model). Section 6 is devoted to the conclusions. Throughout this paper, we adopt the Hubble parameter $H_0 = 75$ km s^{-1} Mpc^{-1} and the deceleration parameter $q_0 = 0.5$ and have converted the results from published papers to this cosmology to facilitate comparisons.

2. SAMPLE SELECTION

The aim of our study is to clear up whether type I ULIRGs are really the transition phase from ULIRGs into QSOs. To accomplish this, we need to use a type I ULIRG sample because the FWHM (Hβ), the optical luminosity at 5100 Å in the rest frame, and the R-band absolute magnitude of host bulges are coeval in these objects. For comparison, we also compile an optically selected QSO sample and an elliptical galaxy sample, for which the BH mass and the R-band absolute magnitude of the bulge are available. The details of these samples are given as follows.

1. The type I ULIRG sample is from Zheng et al. (2002). This sample was compiled from ULIRGs in the QDOT (Queen Mary and Westfield College, Durham, Oxford and Toronto) redshift survey (Lawrence et al. 1999), the 1 Jy ULIRG survey (Kim & Sanders 1998), and an IR QSO sample selected from the cross-correlation of the *IRAS* Point-Source Catalog with the *ROSAT* (*Röntgensatellit*) All-Sky Survey catalog (Boller et al. 1992). All the type I ULIRGs selected by Zheng et al. (2002) are ULIRGs with mid-infrared to far-infrared properties from *IRAS* observations. From this sample, we choose all eight type I ULIRGs (IRAS F07599+6508, IRAS F11119+3257, IRAS Z11598−0112, IRAS F13342+3932, IRAS F15462−0450, IRAS F21219−1757, Mrk 231, and Mrk 1014) for which we have data of the width of the broad Hβ line, the luminosity at 5100 Å, and the R-band absolute magnitude of the host galaxy, M_R(bulge). Therefore, these objects are the best and maximal sample for achieving our aim at this time. For the eight type I ULIRGs, we obtain the FWHM (Hβ) and the optical luminosity at 5100 Å in the rest frame by Zheng et al. (2002) and M_R(bulge) by Veilleux et al. (2002). In the latter paper, the contribution from the R-band absolute magnitude of AGNs was removed for M_R(bulge) (see Veilleux et al. 2002 for this procedure). In addition, according to Veilleux et al. 2002, all eight type I ULIRGs are single-nucleus objects. In the Zheng sample, 23 of 25 type I ULIRGs have an optical luminosity at 5100 Å and the width of the broad Hβ line. Then we compared the eight selected objects with the remaining 15 objects for these two properties. Figure 1

[1] The radiation drag in the solar system is known as the Poynting-Robertson effect. Note that in the early universe, the Compton drag force has a similar effect on the formation of massive BHs (Umemura et al. 1993).

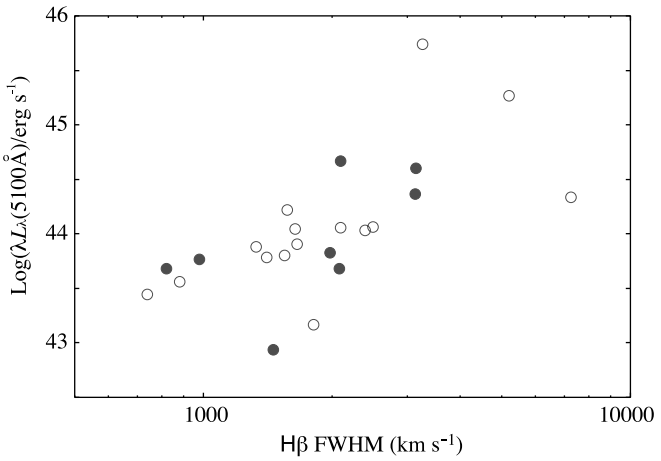

FIG. 1.—Optical luminosity at 5100 Å vs. width of broad Hβ line. The distribution of the eight selected type I ULIRGs (*filled circles*) is similar to that of the remaining 15 type I ULIRGs (*open circles*). [*See the electronic edition of the Journal for a color version of this figure.*]

shows the optical luminosity at 5100 Å against the width of the broad Hβ line. The filled circles denote the eight selected type I ULIRGs, while the open circles represent the remaining 15 type I ULIRGs whose bulge luminosities were not available. As seen in this figure, the eight selected type I ULIRGs could be representative of a large population with respect to the optical luminosity at 5100 Å and the width of the broad Hβ line. In addition, between our sample and the rest we find no significant differences in the ranges of the redshift ($0.1 < z < 0.4$) and infrared luminosity ($L_{\rm IR} > 10^{12}\ L_{\odot}$).

2. The optically selected QSO sample comprises 29 Palomar Green quasars (PG QSOs) from 30 luminous quasars ($M_V < -23$) described by McLure & Dunlop (2001). This QSO sample consists of two optically matched subsamples of 17 radio-quiet QSOs and 13 radio-loud QSOs. The advantage of this sample is that all members have accurate bulge luminosities available from two-dimensional modeling of *Hubble Space Telescope* (*HST*) images. The average redshift of the QSO sample is around 0.2. In this paper, we excluded PG 0157+001 (Mrk 1014) from the optically selected QSO sample, since it is categorized by type I ULIRGs. All 29 QSOs have data of the BH mass and *R*-band magnitude of the bulge compiled by McLure & Dunlop (2001) and Dunlop et al. (2003). In both papers, the contribution from the *R*-band absolute magnitude of AGNs was also removed for M_R(bulge). For 13 PG QSOs in our sample, the infrared flux was taken from Sanders et al. (1989) and Haas et al. (2000, 2003).

3. The elliptical galaxy sample consists of 20 objects drawn from the list of 37 nearby inactive galaxies with dynamical BH measurements published by Kormendy & Gebhardt (2001). In this paper, our main purpose is to investigate the physical link between type I ULIRGs, QSOs, and elliptical galaxies. Thus, we excluded those galaxies in the Kormendy & Dunlop list that were not of E-type morphology (including lenticular galaxies). The Kormendy & Gebhardt list is made up of 20 E-type galaxies. All 20 elliptical galaxies have data of the BH mass and the *B*-band absolute magnitude of the bulge (Kormendy & Gebhardt 2001; Gebhardt et al. 2003). To convert the *B*-band magnitude to the *R* band, standard bulge colors of $B - R = 1.57$ were assumed (Fukugita et al. 1995).

We summarize the various physical parameters of type I ULIRGs, QSOs, and elliptical galaxies in Table 1.

3. BLACK HOLE ESTIMATE OF TYPE I ULIRGs

As mentioned § 2, the BH masses of QSOs and elliptical galaxies have already been estimated by previous works, but we do not have those for eight type I ULIRGs. Thus, we need to estimate them within the present paper. The method for estimating the mass of a BH is based on the assumption that the motion of ionized gas clouds moving around the black hole is dominated by the gravitational force and the clouds within the broad-line region (BLR) are virialized (e.g., Peterson & Wandel 1999, 2000). Thus, the central black hole mass can be expressed by $M_{\rm BH} \approx R_{\rm BLR} v^2/G$, where v is the velocity dispersion of matter at the size of the broad-line region $R_{\rm BLR}$, which is gravitationally bound to the BH.

Then the central mass can be estimated as

$$M_{\rm BH} = 1.5 \times 10^5 \left(\frac{R_{\rm BLR}}{\text{lt-days}}\right)\left(\frac{v_{\rm FWHM}}{10^3\ \text{km s}^{-1}}\right)^2 M_{\odot}. \quad (1)$$

The velocity dispersion v can be estimated from the FWHM of the Hβ broad-line emission $v = f v_{\rm FWHM}$ by assuming that the BLR gas is in isotropic motion ($f = \sqrt{3}/2$). Based on 17 Seyfert galaxies and 17 optically selected PG QSOs, Kaspi et al. (2000) determine an empirical relationship between the size of the broad-line region, $R_{\rm BLR}$, and the optical continuum luminosity, $\lambda L_{\lambda}(5100\ \text{Å})_{\rm rest}$, where $R_{\rm BLR}$ is the distance of the emission-line clouds responding to the central continuum variation as determined from reverberation mappings (see Kaspi et al. 2000):

$$R_{\rm BLR} = 32.9^{+2.0}_{-1.9}\left[\frac{\lambda L_{\lambda}(5100\ \text{Å})_{\rm rest}}{10^{44}\ \text{ergs s}^{-1}}\right]^{0.70\pm0.033} \text{lt-days}. \quad (2)$$

By combining equations (1) and (2), we can obtain the following formula:

$$M_{\rm BH} = 4.9^{+0.4}_{-0.3} \times 10^6 \left[\frac{\lambda L_{\lambda}(5100\ \text{Å})_{\rm rest}}{10^{44}\ \text{ergs s}^{-1}}\right]^{0.70\pm0.033} \times \left(\frac{v_{\rm FWHM}}{10^3\ \text{km s}^{-1}}\right)^2 M_{\odot}. \quad (3)$$

As seen from equation (3), the luminosity at 5100 Å in the rest frame and the FWHM of Hβ are needed to estimate a BH mass. We should also keep in mind that equation (2) holds not only for broad-line type I AGNs but also for NLS1's (Peterson et al. 2000).

In order to evaluate the optical luminosity at 5100 Å in the rest frame, $L_{\lambda}(5100\ \text{Å})_{\rm rest}$, we use the formula $L_{\lambda}(5100\ \text{Å})_{\rm rest} = 4\pi d_L^2 (1+z) F_{\lambda}(5100(1+z)\ \text{Å})_{\rm obs}$, where d_L is the luminosity distance, which is given by $d_L = (cz/H_0)(1 + z/4)$ for a small value of z. Here the FWHM (Hβ) and the observed flux at 5100 Å, $F_{\lambda}(5100(1+z)\ \text{Å})_{\rm obs}$, are given by Zheng et al. (2002) and are measured directly from their spectra.

In this paper, we assume that the contribution from central AGNs dominates the optical emission at 5100 Å in the rest frame and that the stellar continuum emission is negligible. To confirm whether this assumption is reasonable, we check the flux ratio of the optical emission at $5100(1+z)$ Å and the hard X-ray emission at $2-10(1+z)$ keV for five type I ULIRGs. We get the hard X-ray flux from Anabuki (2004). As a consequence, three objects (IRAS F11119+3257, IRAS Z11598−0112, and Mrk 1014) have nearly the same flux ratio as that of PG QSOs, $F_{2-10(1+z)\,\text{keV}}/F_{5100(1+z)\,\text{Å}} = 10^3 - 10^5$. As for PG QSOs, we obtain this flux ratio from the data of $F_{2-10(1+z)\,\text{keV}}$ (George

TABLE 1

THE VARIABLE PHYSICAL PARAMETERS

Name (1)	$\log (M_{BH}/M_{\odot})$ (2)	M_R(host) (mag) (3)	$\log (L_{FIR}/L_{\odot})$ (4)	References (5)
Type I ULIRGs				
IRAS F01572+0009 (Mrk 1014)	7.78	−23.76	12.30	1, 2
IRAS F07599+6508	8.08	−24.68	12.10	1, 2
IRAS F11119+3257	7.11	−22.61	12.29	1, 2
IRAS Z11598−0112	6.28	−22.61	11.56	1, 2
IRAS F12540+5708 (Mrk 231)	7.92	−22.49	12.25	1, 2
IRAS F13342+3932	6.49	−22.87	12.14	1, 2
IRAS F15462−0450	6.26	−20.91	12.00	1, 2
IRAS F21219−1757	7.08	−22.11	11.67	1, 2
PG QSOs				
PG 0137+012	8.58	−23.16	...	3
PG 0736+017	8.01	−22.70	...	3
PG 1004+130	9.11	−23.22	<11.76	3, 4
PG 1020−103	8.37	−22.48	...	3
PG 1217+023	8.42	−22.83	...	3
PG 1226+023	8.62	−23.52	12.12	5, 6
PG 1302−102	8.31	−22.62	12.09	5, 7
PG 1545+210	8.94	−22.42	<11.38	4, 5
PG 2135−147	8.95	−22.62	...	3
PG 2141+175	8.75	−22.92	...	3
PG 2247+140	7.60	−22.92	...	3
PG 2349−014	8.79	−23.52	<11.57	3, 4
PG 2355−082	8.40	−22.72	...	3
PG 0052+251	8.29	−22.12	...	3
PG 0054+144	8.91	−22.72	...	3
PG 0204+292	6.68	−22.42	...	3
PG 0205+024	7.86	−20.22	...	3
PG 0244+194	8.05	−21.89	...	3
PG 0923+201	8.95	−22.37	<11.91	3, 4
PG 0953+414	8.40	−21.98	...	3
PG 1012+008	7.80	−21.90	<11.48	3, 4
PG 1029−140	9.09	−22.12	...	5
PG 1116+215	8.22	−22.82	<11.52	5, 6
PG 1202+281	8.30	−21.92	<11.38	5
PG 1307+085	7.86	−22.02	11.32	5, 7
PG 1309+355	8.01	−22.12	<11.41	5, 6
PG 1402+261	7.30	−20.92	11.39	5, 6
PG 1444+407	8.08	−22.02	11.57	5, 6
PG 1635+119	8.11	−22.17	...	3
Elliptical Galaxies				
NGC 821	7.57	−21.94	...	8
NGC 2778	7.15	−20.12	...	8
NGC 3377	8.00	−20.58	...	8
NGC 3608	8.28	−21.39	...	8
NGC 4291	8.49	−21.16	...	8
NGC 4473	8.04	−21.42	...	8
NGC 4564	7.75	−20.45	...	8
NGC 4649	9.30	−22.83	...	8
NGC 4697	8.23	−21.77	...	8
NGC 5845	8.38	−20.25	...	8
M32	6.59	−17.36	...	9
NGC 3379	8.00	−21.47	...	9
NGC 4486B	8.70	−18.30	...	9
NGC 4742	7.15	−20.47	...	9
NGC 4261	8.71	−22.62	...	9
NGC 4374	8.64	−22.89	...	9
M87	9.48	−23.06	...	9
NGC 6251	8.78	−23.34	...	9
NGC 7052	8.51	−22.84	...	9
IC 1459	8.30	−22.92	...	9

NOTE.—Col. (1): source name; col. (2): BH mass; col. (3): *R*-band absolute magnitude of host galaxies; col. (4): far-infrared luminosity.

REFERENCES (col. [5]).—(1) Zheng et al. 2002; (2) Veilleux et al. 2002; (3) Dunlop et al. 2003; (4) Sanders et al. 1989; (5) McLure & Dunlop 2001; (6) Haas et al. 2003; (7) Haas et al. 2000; (8) Gebhardt et al. 2003; (9) Kormendy & Gebhardt 2001.

TABLE 2
THE BASIC PHYSICAL PARAMETERS OF TYPE I ULIRGS

IRAS Source (1)	z (2)	$F_\lambda(5100(1+z)\ \text{Å})_{\rm obs}$ (ergs s^{-1} cm^{-2} Å^{-1}) (3)	FWHM (Hβ) (km s^{-1}) (4)	$\lambda L_\lambda(5100\ \text{Å})_{\rm rest}$ (ergs s^{-1}) (5)	$F_{2-10(1+z)\,\rm keV}/F_{5100(1+z)\,\text{Å}}$ (6)
IRAS F01572+0009 (Mrk 1014)	0.163	1.41×10^{-15}	2100	4.6×10^{44}	5.3×10^{3}
IRAS F07599+6508	0.148	1.50×10^{-15}	3150	3.9×10^{44}	9.3×10^{1}
IRAS F11119+3257	0.189	1.45×10^{-16}	1980:	6.7×10^{43}	9.0×10^{4}
IRAS Z11598−0112	0.151	1.72×10^{-16}	820	4.7×10^{43}	1.9×10^{4}
IRAS F12540+5708 (Mrk 231)	0.042	1.25×10^{-14}	3130	2.3×10^{44}	3.4×10^{2}
IRAS F13342+3932	0.179	1.44×10^{-16}	980	5.6×10^{43}	...
IRAS F15462−0450	0.101	7.40×10^{-17}	1460	8.6×10^{42}	...
IRAS F21219−1757	0.113	3.24×10^{-16}	2080	8.0×10^{43}	...

NOTES.—The prefix of the object name indicates the origin of *IRAS* fluxes. "F" refers to the *IRAS* Faint Source Catalog, and "Z" means the Faint Source Reject File. The uncertainty on the FWHM is typically of the order of 10%; the colon indicates a value with a relative uncertainty of 20% (Zheng et al. 2002). Col. (1): source name; col. (2): redshift; col. (3): observed flux at $5100(1+z)$ Å; col. (4) FWHM of Hβ emission profile; col. (5): continuum luminosity at the rest frame; col. (6): flux ratio $F_{2-10(1+z)\,\rm keV}/F_{5100(1+z)\,\text{Å}}$; $F_{2-10\,\rm keV(1+z)}$ in units of ergs s^{-1} cm^{-2} Å^{-1}.
REFERENCES.—Cols. (1)–(5): Zheng et al. 2002 and their original spectra. Col. (6): George et al. 2000.

et al. 2000) and $F_{5100(1+z)\,\text{Å}}$ (Kaspi et al. 2000). Although two other objects (IRAS F07599+6508 and Mrk 231), which are broad absorption line QSOs (BAL QSOs), have an extremely low luminosity at the X-ray band, it is believed that this is not due to an intrinsic effect but rather to an absorption effect (e.g., Gallagher et al. 2002). Thus, it is expected that these two BAL QSOs have almost the same flux ratio as that of PG QSOs intrinsically. Since the contributions from AGNs dominate the optical emission for PG QSOs, it is a valid assumption that the central AGNs in type I ULIRGs dominantly power the optical emission at 5100 Å in the rest frame. All the basic parameters of the eight type I ULIRGs are listed in Table 2.

4. RESULTS

4.1. $M_{\rm BH}$-M_R Relation

Figure 2 plots the R-band absolute magnitude of bulge components (spheroidal components), M_R(bulge) (mag), versus the black hole mass, $M_{\rm BH}$ ($M_\odot$), for eight type I ULIRGs, 29 QSOs, and 20 elliptical galaxies. In this figure, the dark gray circles represent type I ULIRGs, the squares show QSOs, and the light gray circles denote elliptical galaxies. The solid line is the best-fitting relation for QSOs. This relation is given by $\log(M_{\rm BH}/M_\odot) = (-0.61 \pm 0.08)M_R(\text{mag}) - (5.47 \pm 1.82)$, which is comparable to that found by Laor (1998). The underscored object names denote objects whose properties at the soft and hard X-ray bands are similar to those of NLS1's (Anabuki 2004). For all QSOs and elliptical galaxies, the effect of Galactic and internal extinction has been corrected (McLure & Dunlop 2001; Dunlop et al. 2003; Gebhardt et al. 2003; Kormendy & Gebhardt 2001). In the case of type I ULIRGs, the effect of the visual extinction may not be negligible because of significantly larger FIR luminosity, which would imply plenty of dusty gas. Thus, the optical extinction may affect the estimation of the BH masses and the bulge luminosities. Then we exhibit the extinction effect toward the BLRs of type I ULIRGs (Fig. 2, *arrows*). Hereafter, we use A_V as the total extinction toward the BLRs of type I ULIRGs. In addition, the effect of optical extinction for the hosts of type I ULIRGs may also be significant (e.g., Veilleux et al. 2002). If this is the case, then we are underestimating the bulge luminosity of type I ULIRGs. As for the morphology of host galaxies, several works have showed that the surface brightness profiles of QSO hosts resemble a de Vaucouleurs profile (e.g., McLure et al. 1999). As for the eight type I ULIRGs, the surface brightness profiles of six host galaxies in type I ULIRGs can be fitted with a de Vaucouleurs profile (elliptical-like) for the R and K' bands, and the others (IRAS 11598 and IRAS F15462) can be fitted with both a de Vaucouleurs profile and an exponential profile (disklike) for their band (Veilleux et al. 2002). Thus, in Figure 2 we use the label "(E/D)" for the latter two objects. In this paper, we focus on the absolute magnitude of their spheroidal components. If the magnitudes of galaxies are dominated by disk components, our estimates of the R-band absolute magnitude in bulges would be overestimated. Note that we assume $f = \sqrt{3}/2$ to estimate the BH mass for QSOs, while McLure & Dunlop used $f = 3/2$, and thus our estimate for QSO BHs is 3 times as small as their estimate.

As seen in Figure 2, we have found that type I ULIRGs have systematically smaller BH mass than do QSOs and elliptical

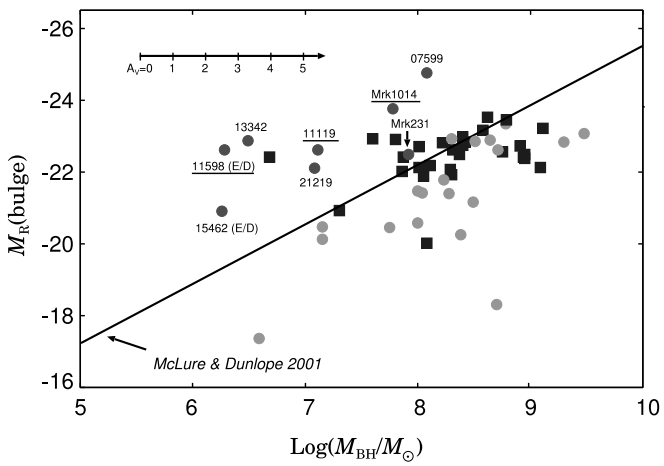

FIG. 2.—Absolute R-band bulge magnitude vs. black hole mass for eight type I ULIRGs (*dark gray circles*), 29 QSOs (*squares*), and 20 elliptical galaxies (*light gray circles*). The black hole masses for type I ULIRGs are derived from their broad Hβ line widths by using eq. (3). The black hole masses for QSOs are given by McLure & Dunlop (2001) and Dunlop et al. (2003). The black hole masses for elliptical galaxies are the dynamical estimates of Kormendy & Gebhardt (2001) and Gebhardt et al. (2003). The black horizontal arrow shows the extinction effects for the BLR of type I ULIRGs. Underscored objects have the same properties at the hard X-ray band as NLS1's (Anabuki 2004). The solid line is the best-fitting relation for the optical QSOs, which is $\log(M_{\rm BH}/M_\odot) = (-0.61 \pm 0.08)M_R(\text{mag}) - (5.47 \pm 1.82)$. "(E/D)" denotes objects that can be fitted with both a de Vaucouleurs profile (elliptical-like) and an exponential profile (disklike) for the R and K' bands (Veilleux et al. 2002). [*See the electronic edition of the Journal for a color version of this figure.*]

galaxies in spite of the comparable bulge luminosity, if the visual extinction effect is small ($A_V < 3$) for type I ULIRGs. Namely, the BH mass ranges are $M_{\rm BH} \approx 10^6-10^8\ M_\odot$ for type I ULIRGs and $M_{\rm BH} \approx 10^8-10^9\ M_\odot$ for QSOs and elliptical galaxies. However, if A_V of all type I ULIRGs is larger than $\sim$3, the BH mass of type I ULIRGs would be similar to that of QSOs. Thus, in order to be confident that the BH mass of type I ULIRGs is systematically small, we need to constrain the effect of visual extinction, which is discussed in § 4.3. On the other hand, if the extinctions for their host galaxies are significant, then the data points just move upward in Figure 2. In short, this effect makes the difference between the BH mass distributions of type I ULIRGs, QSOs, and elliptical galaxies large. In addition, we find that the elliptical galaxies have slightly lower y-values than QSOs in Figure 2. According to KUM03, this result may indicate that the hosts of QSOs are slightly younger than those of elliptical galaxies (for details, see § 5).

Finally, we check the effects of systematic errors in the methods used to evaluate BH masses and the effect of our sample bias. First, we discuss the systematic errors in the methods. For the type I ULIRGs, the uncertainties of the BH mass were estimated by error propagation using the optical luminosity at 5100 Å and the FWHM of the Hβ measurements given by Zheng et al. (2002). The mean error of the BH mass is a factor of 1.3. Although McLure & Dunlop (2001) did not show the uncertainties of BH masses clearly, in general the BH mass computed in this way (see § 3) is accurate to within a factor of 2–3 (e.g., Wang & Lu 2001; Marziani et al. 2003; Shemmer et al. 2004). As seen in Figure 2, except for Mrk 231, the BH masses of type I ULIRGs are 10 times as small as those of QSOs and elliptical galaxies at the fixed R-band magnitude of the bulge. Furthermore, the mean error of the BH mass for elliptical galaxies is a factor of 3. Thus, it is clear that the systematic difference of BH masses between type I ULIRGs and QSOs (or elliptical galaxies) cannot be explained by only systematic errors in methods of BH mass measurement. On the other hand, as shown in § 2, the eight selected type I ULIRGs could be representative of a large population. Thus, the range of BH masses in the 12 other type I ULIRGs is similar to that of the eight selected type I ULIRGs with $M_{\rm BH} = 10^6-10^8\ M_\odot$. The remaining three objects have massive BHs with $\approx 10^9\ M_\odot$. As a consequence, 12 type I ULIRGs would be located the farthest from the location of the QSOs if the range of bulge R-band magnitude is from -22 to -24, which is the typical range for the eight selected type I ULIRGs. Thus, we found that the systematic difference that we found in the M_R(bulge)-$M_{\rm BH}$ diagram would not be an effect of our sample bias. We should keep in mind that other results that we show (Figs. 2 and 3) also do not change significantly as a result of the systematic errors in the BH measurements and the effect of our sample bias.

4.2. $M_{\rm BH}$-$L_{\rm FIR}$ *Relation*

Figure 3 shows the BH mass–to–FIR luminosity relation $M_{\rm BH}$-$L_{\rm FIR}$(40–500 μm) using the derived BH mass (see Table 1) and the FIR luminosity for eight type I ULIRGs (Zheng et al. 2002). In order to compare the result for type I ULIRGs with that for QSOs, we select 13 PG QSOs from the sample selected by McLure & Dunlop (2001) and Dunlop et al. (2003). All 13 PG QSOs have data for the *IRAS* flux densities at 60 and 100 μm (Sanders et al. 1989; Haas et al. 2000, 2003). For the 13 PG QSOs, we calculated their far-infrared luminosities with the following formula (Sanders & Mirabel 1996), based on the flux densities from the *IRAS* Faint Source Catalog: $L_{\rm FIR}(40-500\ \mu{\rm m}) = 4\pi d_L^2 C F_{\rm FIR}$, where the scale factor C (=1.4–1.8) is the correction factor required to account principally for extrapolated flux longward of the *IRAS* 100 μm filter, and $F_{\rm FIR}$ is defined as $1.26\times10^{-14}(2.58 f_{60} + f_{100})$(W m^{-2}), where f_{60} and f_{100} are the *IRAS* flux densities at 60 and 100 μm in units of janskys. Here we employ $C = 1.8$. The circles show the type I ULIRGs, and the squares and arrows represent QSOs. The horizontal arrow shows the optical extinction effect for the BLRs of type I ULIRGs. The thick solid line denotes a luminosity ratio of far-infrared to Eddington luminosity ($L_{\rm FIR}/L_{\rm Edd}$) equal to unity. The thin solid, dashed, and dot-dashed lines represent $L_{\rm FIR}/L_{\rm Edd} =$ 10, 0.1, and 0.01, respectively.

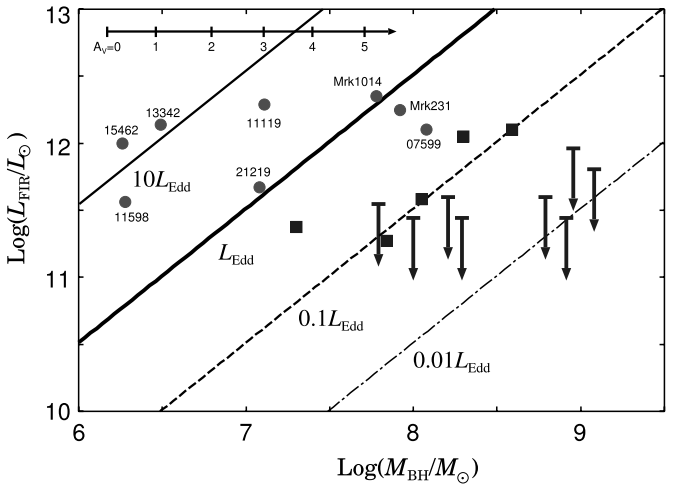

FIG. 3.—Far-infrared luminosity vs. black hole mass for eight type I ULIRGs (*circles*) and 13 PG QSOs (*squares and arrows*). The black horizontal arrow shows the effect of visual extinction for the BLRs of type I ULIRGs. The thick solid line denotes the luminosity ratio of far-infrared to Eddington luminosity ($L_{\rm FIR}/L_{\rm Edd}$) equal to unity. The thin solid, dashed, and dot-dashed lines show $L_{\rm FIR}/L_{\rm Edd} = 10$, 0.1, and 0.01, respectively. [*See the electronic edition of the Journal for a color version of this figure.*]

As seen in Figure 3, it turns out that the FIR luminosity is larger than the Eddington luminosity for most type I ULIRGs in Figure 3. By contrast, the FIR luminosity is more than 1 order of magnitude smaller than the Eddington luminosity for QSOs, namely $L_{\rm FIR} < 0.1 L_{\rm Edd}$. This may indicate AGNs in type I ULIRGs with a high mass accretion rate, or the existence of another power source, for which the most promising candidate is a starburst. We discuss this issue in § 5.1. In addition, Figure 3 shows that type I ULIRGs systematically have a smaller BH mass than QSOs at a fixed FIR luminosity. On the other hand, the large far-infrared luminosity would imply the plenty of dusty gas (e.g., Haas et al. 2003). Hence, for type I ULIRGs this shows that the mass ratios of the total dusty gas to the BH are much larger than those of QSOs. It would indicate that BH masses of type I ULIRGs have growth potential.

4.3. *Optical Extinction Effect*

As mentioned in §§ 4.1 and 4.2, we found that type I ULIRGs have systematically smaller BHs than those of QSOs given the absolute magnitude of the bulge and given the FIR luminosity. However, the BH masses of type I ULIRGs depend on the optical extinction effect, namely, the heavy extinction makes the derived BH mass smaller (see the horizontal arrow in Figs. 2 and 3). On the other hand, it is well known that the Balmer decrement is a standard method of evaluating the optical extinction of narrow-line regions (e.g., Osterbrock 1989). However, this method is generally invalid for estimating the amount of visual extinction toward BLRs because the flux ratios of broad

TABLE 3
THE PARAMETERS FOR THE EXTINCTION OF TYPE I ULIRGS

IRAS Source (1)	$N_{\rm H}$ ($\rm cm^{-2}$) (2)	A_V (mag) (3)	$A_V^{\rm Galactic}$ (mag) (4)	Reference (5)
IRAS F01572+0009 (Mrk 1014)	$<2.6 \times 10^{20}$	<0.012	0.087	1
IRAS F07599+6508	$>10^{24}$	...	0.16	2
IRAS F11119+3257	1.2×10^{22}	0.57	0.159	1
IRAS Z11598−0112	6×10^{20}	0.029	0.066	1
IRAS F12540+5708 (Mrk 231)	$>10^{24}$	...	0.078	3
IRAS F13342+3932	...	...	0.012	...
IRAS F15462−0450	...	...	0.65	...
IRAS F21219−1757	...	...	0.21	...

NOTES.—Col. (1): source name. Col. (2): column density. Col. (3): internal optical extinctions derived from column density. The value is evaluated by $A_V/N_{\rm H} = 4.8^{+14.1}_{-3.6} \times 10^{-23}$ mag $\rm cm^{-2}$ (1 σ dispersion) derived from AGN observation (Maiolino et al. 2001a). Col. (4): Galactic extinction at the visual band.
REFERENCES.—(1) Anabuki 2004; (2) Imanishi & Terashima 2004; (3) Braito et al. 2004.

Balmer lines are sometimes seriously affected by collisional excitation effects. As a complementary approach, the hard X-ray observations enable us to make a measurement of the extinction toward the nucleus and to constrain the BH mass more reliably. We should note that many observations have suggested that the absorption column density ($N_{\rm H}$) derived from hard X-rays is systematically large relative to the optical extinction of A_V under the assumption of a Galactic gas/dust mass ratio (e.g., Maiolino et al. 2001b; Watanabe et al. 2004). Thus, we estimate the optical extinction of three type I ULIRGs (IRAS F11119+3257, IRAS Z11598−0112, and Mrk 1014) with the relation $A_V/N_{\rm H} = 4.8^{+14.1}_{-3.6} \times 10^{-23}$ mag $\rm cm^{-2}$ (1 σ dispersion), which is derived from the AGN observations (Maiolino et al. 2001a). As for the two BAL QSOs (IRAS F07599+6508 and Mrk 231), the $A_V/N_{\rm H}$ relation for normal QSOs would not hold for BAL QSOs. However, recent works have found that the optical extinction of BAL QSOs is around 0.1–1 by comparing the composite non-BAL QSO spectra with the composite BAL QSO spectra (e.g., Brotherton et al. 2001; Reichard et al. 2003). Therefore, the optical extinction of the two BAL QSO in our sample may be less than $A_V = 1$. We summarize the visual extinctions for type I ULIRGs in Table 3. For at least three type I ULIRGs for which we are able to estimate the visual extinction from the column density, we show that our results (§§ 4.1 and 4.2) do not change drastically.

4.4. *Summary of Observational Results*

Based on the above results, we summarize our findings on type I ULIRGs as follows. (1) The BH mass of type I ULIRGs is systematically smaller than that of QSOs and elliptical galaxies despite their comparable bulge luminosities. (2) Most type I ULIRGs have particularly large FIR luminosity compared to the Eddington luminosity. We show that the above results do not change significantly for three type I ULIRGs even if we consider the effects of visual extinction. Also, for eight type I ULIRGs, we investigate the effect of the uncertainty of the BH mass measurements and our sample bias, and we found that our results are not altered. In addition, their X-ray luminosity properties are similar to those of NLS1's, whose X-ray properties reflect a high mass accretion rate (see Anabuki 2004 for details). From all these findings, it would be natural to conclude that type I ULIRGs are the early phase of BH growth, namely, the transition stage from ULIRGs to QSOs. In the next section, we investigate whether this interpretation is reasonable by comparing our results with the theoretical prediction.

5. DISCUSSIONS

Based on our observational results for eight type I ULIRGs, we have suggested that type I ULIRGs could be the transition stage from ULIRGs to QSOs. However, it has not yet been made clear what the physical relationship is between type I ULIRGs, QSOs, and elliptical galaxies with the objective of elucidating the coevolution of host galaxies and SMBHs. For this purpose, we compare our results with the theoretical predictions of a coevolution scenario for galactic bulges and SMBHs.

5.1. *A Coevolution Scheme for SMBHs and Galactic Bulges*

Recently, KUM03 have constructed a physical model for the coevolution of a QSO BH and an early-type host galaxy. This model is based on the radiation drag incorporating a realistic chemical evolution that reproduces the color-magnitude relation of the present-day bulge. Here we briefly review the essence of their model as a preview of the following discussions. In their model, they used the evolutionary spectral synthesis code PEGASE (Fioc & Rocca-Volmerange 1997) to treat the realistic chemical evolution of the galactic bulges. According to the results of KUM03, after a galactic wind epoch t_w, the bolometric luminosity is shifted from the host-dominant phase to the AGN-dominant phase (the QSO phase) at the transition time $t_{\rm crit}$. The former phase ($t_w < t < t_{\rm crit}$) corresponds to the early stage of a growing BH because the mass accretion rate during this phase is so high that the mass growth of the BH is significant. They defined this phase as a "proto-QSO." The proto-QSO phase is preceded by an optically thick phase before the galactic wind, which would correspond to a classical ULIRG. In this phase, they predicted that the BH is much smaller than in the QSO phase. After the AGN luminosity exhibits a peak at $t_{\rm cross}$, it fades out abruptly because almost all of the matter around the BH has fallen onto the central BH. The fading nucleus could be a low-luminosity AGN (LLAGN).

5.2. *Are Type I ULIRGs the Missing Link between ULIRGs and QSOs?*

By using the KUM03 model, we predict the evolution of M_R(bulge) and $M_{\rm BH}$ for the different masses of the bulges in

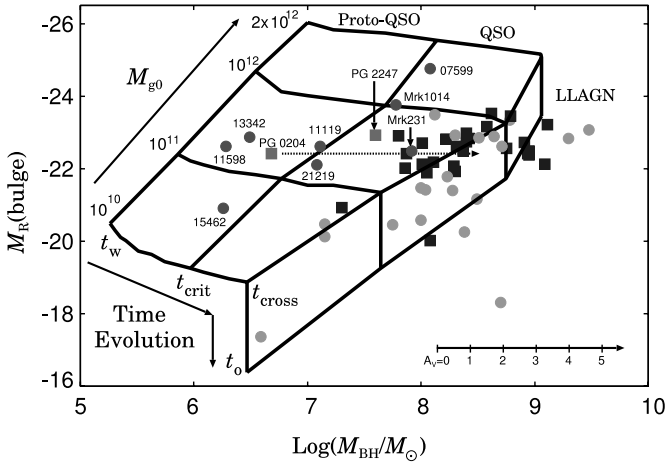

FIG. 4.—Absolute *R*-band bulge magnitude vs. black hole mass for eight type I ULIRGs (*red circles*), 27 QSOs (*squares*), two "unusual" QSOs (*squares*), and 20 elliptical galaxies (*circles*). The dotted arrow denotes the BH mass if we use the broad line width with 8000 km s^{-1}. The solid horizontal arrow shows the optical extinction for the BLR of type I ULIRGs. The grid represents the prediction based on the radiation drag model for different masses of bulges ($M_{g0} = 10^{10}$, 10^{11}, 10^{12}, and 2×10^{12} $M_\odot$), where M_{g0} is the initial gas mass in galactic bulges. Each evolution shift is from left (smaller BH) to right (larger BH) in this figure. The quantity t_w is the galactic wind timescale, and t_{crit} is the time when the luminosity of the bulges is equal to that of AGNs. We define t_{cross} as the time when almost all of the matter around the BH has fallen onto the central BH. The quantity t_0 denotes the final stage of galaxy evolution. The host luminosity–dominant phase (proto-QSOs) corresponds to the region $t_w < t < t_{crit}$. The AGN luminosity–dominant phase (QSOs) corresponds to the area $t_{crit} < t < t_{cross}$. We call the phase $t_{cross} < t < t_0$ an LLAGN. [*See the electronic edition of the Journal for a color version of this figure.*]

Figure 4. Here we calculate the evolutional tracks in the M_R-M_{BH} diagram for four different masses of bulges ($M_{g0} = 10^{10}$, 10^{11}, 10^{12}, and 2×10^{12} $M_\odot$), where M_{g0} is the initial gas mass in galactic bulges. In this figure, we assume a Salpeter-type initial mass function (IMF) of $\phi = dn/d \log m_* = A(m_*/M_\odot)^{-1.35}$ for a mass range of [0.1 $M_\odot$, 60 $M_\odot$]. The star formation rate (SFR) per unit mass at time t, $C(t)$, is assumed to be proportional to the gas mass fraction f_g; $C(t) = kf_g$ at $t < t_w$, and at $t \geq t_w$ $C(t) = 0$, where k is the constant rate coefficient. In Table 4, we summarize the model parameters (M_{g0}, k, t_w, t_{crit}, and t_{cross}).[2] The evolutions of different stellar masses of bulges proceed from left (smaller BH) to right (larger BH) in Figure 4. The black horizontal arrow denotes the optical extinction effect for the BLR of type I ULIRGs.

As seen in Figure 4, it is found that most type I ULIRGs are located near the proto-QSO phase. This could indicate that type I ULIRGs are the early phase of BH growth within younger bulges and then they evolve into QSOs. Namely, it suggests that type I ULIRGs are the missing link between ULIRGs and QSOs. In addition, we also find that two "unusual" QSOs (PG 0204+292 and PG 2247+140) are located near the region of the proto-QSOs. In fact, these unusual QSOs have a narrower Hβ line width (<2500 km s^{-1}) among the samples of PG QSOs (McLure & Dunlop 2001). Thus, these may correspond to objects in the process of evolving into QSOs. However, as for PG 0204+140, we should comment that it has not only a strong narrow component, but also a very broad line width (about 8000 km s^{-1}; see Fig. 6 in McLure & Dunlop 2001). If we estimate its BH mass by using a larger FWHM, PG 0204+140 has a BH mass of 3×10^8 $M_\odot$ (Fig. 4, *dotted arrow*). If this is the case, it is located near the region of normal QSOs in Figure 4. In addition, our model can explain the difference from QSOs and elliptical galaxies as the evolution of host galaxies with nearly the same BH mass. Moreover, according to KUM03, it would be expected that the parent galaxies of type I ULIRGs are starburst galaxies, in which there is some AGN activity. This corresponds to classical ULIRGs. In this phase, their BH mass would be much smaller than the BH mass of type I ULIRGs. To sum up, we found that classical ULIRGs → type I ULIRGs → QSOs → elliptical galaxies would be explained by the evolution sequence of spheroidal systems. However, there are some discrepancies between the predictions of the KUM03 model and our results for the type I ULIRGs. In KUM03, they predicted that a proto-QSO is *optically thin and the total luminosity is still dominated by the host components*. On the other hand, for type I ULIRGs, we revealed the following: (1) The AGNs power the optical emission rather than the stellar components (see § 3). This might imply that AGNs contribute the energy source of FIR luminosity. (2) An FIR luminosity larger than the Eddington luminosity indicates that the optical depth of their hosts is still thick (§ 4.2). It is useful to consider the reasons for these two disagreements. Hence, we discuss this in the following sections.

TABLE 4
THE BASIC MODEL PARAMETERS (KUM03 MODEL)

M_{g0} ($M_\odot$) (1)	k (Gyr^{-1}) (2)	t_w (yr) (3)	t_{crit} (yr) (4)	t_{cross} (yr) (5)
10^{10}	14.7	1.3×10^8	4.5×10^8	7×10^8
10^{11}	11.3	3.5×10^8	8×10^8	1.2×10^9
10^{12}	8.6	7×10^8	1.2×10^9	1.8×10^9
2×10^{12}	8.1	8×10^8	1.4×10^9	2×10^9

NOTES.—Col. (1): Initial gas mass in galactic bulges. Col. (2): Constant rate coefficient for the SFR. Col. (3): Galactic wind timescale. Col. (4): Transition time from the host luminosity–dominant phase to the AGN luminosity–dominant phase. Col. (5): Time when the BH growth stops. For more information about these parameters, see also text and the original paper (KUM03).

5.2.1. *Origin of the FIR Luminosity*

In the KUM03 model, they assume the AGN luminosity to be the Eddington luminosity. However, recent optical and X-ray observations have suggested that almost all type I ULIRGs are in high mass accretion phases (Anabuki 2004; Hao et al. 2005). If the accretion rate onto a BH is super-Eddington ($\dot{M} > \dot{M}_E$), then the solution of accretion is optically thick and called a *slim disk* (e.g., Abramowicz et al. 1988), where the Eddington accretion rate $\dot{M}_E = L_E/c^2$ (e.g., Kato et al. 1998). In this type of disk, the photon-trapping effect (e.g., Katz 1977; Begelman 1978) in the accretion flow plays an important role. In fact, the BH accretion luminosity can achieve up to $\approx 10 L_E$ (Ohsuga et al. 2002, 2003, 2005). Hence, by considering such a super-Eddington accretion in type I ULIRGs, it is expected that the AGN luminosity becomes larger than the host luminosity, and then this may be consistent with the observational result. If this is the case, moreover, it then turns out that the FIR luminosity of type I ULIRGs can be explained by only the BH accretion luminosity (see thin solid line, $L_{FIR}/L_{Edd} = 10$, in Fig. 3). On the other hand, recent high-resolution multiwavelength observations have indicated that the vast majority of ULIRGs are

[2] As for the effect of the star formation history, if the mass range and slope of the IMF and the SFR are changed to satisfy the spectrophotometric properties of galactic bulges, the final BH mass is altered by a factor of ±50% (Kawakatu & Umemura 2004).

strongly interacting or merging galaxies (e.g., Clements et al. 1996; Murphy et al. 1996; Veilleux et al. 2002). Thus, such an interaction or merger may cause a starburst (e.g., Larson & Tinsley 1978; Noguchi 1988; Mihos & Hernquist 1994; Sanders & Mirabel 1996), and thus a starburst phenomenon may contribute to the FIR luminosity of type I ULIRGs. However, there is plenty of scope for discussion about whether the interactions or mergers trigger the starbursts, as Bergvall et al. (2003) claimed that the interactions and mergers do not trigger the starburst. Nevertheless, it is worth emphasizing again that the AGN luminosity can produce the FIR luminosity of type I ULIRGs only if the accretion rate is $\dot{M} > \dot{M}_{\rm E}$. This would affect one of the important issues for ULIRGs, that is, whether the dominant energy sources of ULIRGs are dust-obscured AGNs or starbursts.

5.2.2. *Obscuring Problem*

KUM03 was based on a monolithic model for the coevolution of an SMBH and a galaxy. As we mentioned in § 5.2.1, however, almost all ULIRGs have undergone mergers or interactions, and also the AGN phenomenon appears at the final merging stage (e.g., Clements et al. 1996; Kim et al. 1998; Wu et al. 1998; Zheng et al. 1999; Canalizo & Stockton 2001; Cui et al. 2001). Thus, the interactions or mergers would play a significant role in elucidating the physical link between ULIRGs and QSOs. If dusty galaxies interact or merge with optically thin proto-QSOs, then the dusty gas may be wound up and then dust-enshrouded AGNs may form. The objects may seem from observations to be type I ULIRGs. After the dusty gas is swept away by feedback from multiple supernovae and the AGN (e.g., Granato et al. 2004), type I ULIRGs would evolve into optically thin QSOs. Another possibility is that type I ULIRGs may be on the way to blowing away the dusty gas even within the monolithic scenario. Indeed, the duration of sweeping away the dusty gas is finite, so the bulges would be mildly optically thick during this phase, although we supposed that the galactic wind sweeps the dusty gas away instantly in Figure 4. Thus, in order to understand the physical properties of type I ULIRGs in detail, we will elucidate the wind effects and interactions or mergers with dusty galaxies by using sophisticated simulations in future work.

6. CONCLUSIONS

We have investigated whether type I ULIRGs are really in the transition stage from ULIRGs to QSOs, using the data of infrared, optical, and X-ray observations. To reveal this issue, we compare the BH mass, the bulge luminosity, and the FIR luminosity among type I ULIRGs, QSOs, and elliptical galaxies. Our main conclusions are

1. Type I ULIRGs have systematically smaller BH masses in spite of a comparable bulge luminosity relative to QSOs.
2. The far-infrared luminosity of most type I ULIRGs is larger than the Eddington luminosity.
3. We have shown that our results do not change significantly for three type I ULIRGs for which we can evaluate the effects of visual extinction. In addition, we have examined the effect of the uncertainty of the BH mass measurements and our sample bias, and we found that our results do not change drastically.
4. The X-ray properties of type I ULIRGs, which are similar to those of narrow-line Seyfert 1 galaxies (Anabuki 2004), indicate that AGNs with a high mass accretion rate exist in type I ULIRGs.
5. Based on all of these findings (1–4), it would be natural to interpret type I ULIRGs as the early phase of BH growth, namely, the missing link between ULIRGs and QSOs. Moreover, by comparing our results with a theoretical model of a coevolution scenario of a QSO BH and a galactic bulge, we have found that this explanation is reasonable.
6. The AGN luminosity can produce the FIR luminosity of type I ULIRGs only if we use super-Eddington accretion. This result would affect the origin of the infrared luminosity in ULIRGs.

The authors thank the anonymous referee for constructive comments and suggestions. The analysis was made with the computational facilities at the Center for Computational Sciences at the University of Tsukuba. We thank X. Z. Zheng for kindly supplying the observed spectra of type I ULIRGs. We are grateful to M. Akiyama, M. Imanishi, K. Ohsuga, and Y. Terashima for useful comments and discussions. N. K. also acknowledges the Italian Ministero dell'Istruzione dell'Università e della Ricerca (MIUR) and the Istituto Nazionale di Astrofisica (INAF) for financial support. N. A. and T. Nagao acknowledge financial support from the Japan Society for the Promotion of Science (JSPS) through the JSPS Research Fellows. This work is supported in part by a Grant-in-Aid for Scientific Research from the Ministry of Education, Science, Culture, Sports and Technology of Japan (No. 16002003 to M. U.).

REFERENCES

Abramowicz, M. A., Czerny, B., Lasota, J. P., & Szuszkiewicz, E. 1988, ApJ, 332, 646
Alexander, D. M., Smail, I., Bauer, F. E., Chapman, S. C., Blain, A. W., Brandt, W. N., & Ivison, R. J. 2005, Nature, 434, 738
Anabuki, N. 2004, Ph.D. thesis, Univ. Tokyo
Bahcall, J. N., Kirhakos, S., Saxe, D. H., & Schneider, D. P. 1997, ApJ, 479, 642
Begelman, M. C. 1978, MNRAS, 184, 53
Bergvall, N., Laurikainen, E., & Aalto, S. 2003, A&A, 405, 31
Boller, Th., Brandt, W. N., & Fink, H. 1996, A&A, 305, 53
Boller, Th., Meurs, E. J. A., Brinkmann, W., Fink, H., Zimmermann, U., & Adorf, H.-M. 1992, A&A, 261, 57
Borys, C., Smail, I., Chapman, S. C., Blain, A. W., Alexander, D. M., & Ivison, R. J. 2005, ApJ, 635, 853
Braito, V., et al. 2004, A&A, 420, 79
Brotherton, M. S., Tran, H. D., Becker, R. H., Gregg, M. D., Laurent-Muehleisen, S. A., & White, R. L. 2001, ApJ, 546, 775
Brotherton, M. S., et al. 1999, ApJ, 520, L87
Canalizo, G., & Stockton, A. 2001, ApJ, 555, 719
Clements, D. L., Sutherland, W. J., Saunders, W., Efstathiou, G. P., McMahon, R. G., Maddox, S., Lawrence, A., & Rowan-Robinson, M. 1996, MNRAS, 279, 459
Cui, J., Xia, X.-Y., Deng, Z.-G., Mao, S., & Zou, Z.-L. 2001, AJ, 122, 63
Dunlop, S., McLure, R. J., Kukula, M. J., Baum, S. A., O'Dea, C. P., & Hughes, D. H. 2003, MNRAS, 340, 1095
Falomo, R., Kotilainen, J. K., Pagani, C., Scarpa, R., & Treves, A. 2004, ApJ, 604, 495
Fioc, M., & Rocca-Volmerange, B. 1997, A&A, 326, 950
Fukugita, M., Shimasaku, K., & Ichikawa, T. 1995, PASP, 107, 945
Gallagher, S. C., Brandt, W. N., Chartas, G., & Garmire, G. P. 2002, ApJ, 567, 37
Gebhardt, K., et al. 2003, ApJ, 583, 92
George, I. M., Turner, T. J., Yaqoob, T., Netzer, H., Laor, A., Mushotzky, R. F., Nandra, K., & Takahashi, T. 2000, ApJ, 531, 52
Granato, G. L., De Zotti, G., Silva, L., Bressan, A., & Danese, L. 2004, ApJ, 600, 580
Haas, M., Müller, S. A. H., Chini, R., Meisenheimer, K., Klaas, U., Lemke, D., Kreysa, E., & Camenzind, M. 2000, A&A, 354, 453

Haas, M., et al. 2003, A&A, 402, 87
Hao, C. N., Xia, X. Y., Mao, S., Wu, H., & Deng, Z. G. 2005, ApJ, 625, 78
Hooper, E. J., Impey, C. D., & Foltz, C. B. 1997, ApJ, 480, L95
Imanishi, M., & Terashima, Y. 2004, AJ, 127, 758
Joseph, R. D., & Wright, G. S. 1985, MNRAS, 214, 87
Kaspi, S., Smith, P. S., Netzer, H., Maoz, D., Jannuzi, B. T., & Giveon, U. 2000, ApJ, 533, 631
Kato, S., Fukue, J., & Mineshige, S. 1998, Black-Hole Accretion Disks (Kyoto: Kyoto Univ. Press)
Katz, J. I. 1977, ApJ, 215, 265
Kawakatu, N., & Umemura, M. 2002, MNRAS, 329, 572
———. 2004, ApJ, 601, L21
Kawakatu, N., Umemura, M., & Mori, M. 2003, ApJ, 583, 85
Kim, D.-C., & Sanders, D. B. 1998, ApJS, 119, 41
Kim, D.-C., Veilleux, S., & Sanders, D. B. 1998, ApJ, 508, 627
Kirhakos, S., Bahcall, J. N., Schneider, D. P., & Kristian, J. 1999, ApJ, 520, 67
Kormendy, J., & Gebhardt, K. 2001, in AIP Conf. Proc. 586, 20th Texas Symp. on Relativistic Astrophysics, ed. H. Martel & J. C. Wheeler (New York: AIP), 363
Kormendy, J., & Richstone, D. 1995, ARA&A, 33, 581
Laor, A. 1998, ApJ, 505, L83
Larson, R. B., & Tinsley, B. M. 1978, ApJ, 219, 46
Lawrence, A., et al. 1999, MNRAS, 308, 897
Lípari, S., Terlevich, R., Zheng, W., Garcia-Lorenzo, B., Sanchez, S. F., & Bergmann, M. 2005, MNRAS, 360, 416
Maiolino, R., Marconi, A., & Oliva, E. 2001a, A&A, 365, 37
Maiolino, R., Marconi, A., Salvati, M., Risaliti, G., Severgnini, P., Oliva, E., La Franca, F., & Vanzi, L. 2001b, A&A, 365, 28
Marconi, A., & Hunt, L. K. 2003, ApJ, 589, L21
Marziani, P., Zamanov, R. K., Sulentic, J. W., & Calvani, M. 2003, MNRAS, 345, 1133
Mathur, S. 2000, MNRAS, 314, L17
McLeod, K. K., & Rieke, G. H. 1995, ApJ, 454, L77
McLeod, K. K., Rieke, G. H., & Storrie-Lombardi, L. J. 1999, ApJ, 511, L67
McLure, R. J., & Dunlop, J. S. 2001, MNRAS, 327, 199
———. 2002, MNRAS, 331, 795
McLure, R. J., Dunlop, J. S., & Kukula, M. J. 2000, MNRAS, 318, 693
McLure, R. J., Kukula, M. J., Dunlop, J. S., Baum, S. A., O'Dea, C. P., & Hughes, D. H. 1999, MNRAS, 308, 377
Mihos, J. C., & Hernquist, L. 1994, ApJ, 425, L13
Mineshige, S., Kawaguchi, T., Takeuchi, M., & Hayashida, K. 2000, PASJ, 52, 499
Murphy, T. W., Armus, L., Matthews, K., Soifer, B. T., Mazzarella, J. M., Shupe, D. L., Strauss, M. A., & Neugebauer, G. 1996, AJ, 111, 1025
Noguchi, M. 1988, A&A, 203, 259
Ohsuga, K., Mineshige, S., Mori, M., & Umemura, M. 2002, ApJ, 574, 315
Ohsuga, K., Mineshige, S., & Watarai, K. 2003, ApJ, 596, 429
Ohsuga, K., Mori, M., Nakamoto, T., & Mineshige, S. 2005, ApJ, 628, 368
Osterbrock, D. E. 1989, Astrophysics of Gaseous Nebulae and Active Galactic Nuclei (Mill Valley: University Science Books)
Peterson, B. M., McHardy, I. M., & Wilkes, B. J. 2000, NewA Rev., 44, 491
Peterson, B. M., & Wandel, A. 1999, ApJ, 521, L95
———. 2000, ApJ, 540, L13
Pounds, K. A., Done, C., & Osborne, J. P. 1995, MNRAS, 277, L5
Reichard, T. A., et al. 2003, AJ, 126, 2594
Richstone, D., et al. 1998, Nature, 395, A14
Sanders, D. B., & Mirabel, I. F. 1996, ARA&A, 34, 749
Sanders, D. B., Phinney, E. S., Neugebauer, G., Soifer, B. T., & Matthews, K. 1989, ApJ, 347, 29
Sanders, D. B., Soifer, B. T., Elias, J. H., Madore, B. F., Matthews, K., Neugebauer, G., & Scoville, N. Z. 1988, ApJ, 325, 74
Sato, J., Umemura, M., Sawada, K., & Matsuyama, S. 2004, MNRAS, 354, 176
Scoville, N. Z. 1992, in ASP Conf. Ser. 31, Relationships between Active Galactic Nuclei and Starburst Galaxies, ed. A. V. Filippenko (San Francisco: ASP), 159
Shemmer, O., Netzer, H., Maiolino, R., Oliva, E., Croom, S., Corbett, E., & di Fabrizio, L. 2004, ApJ, 614, 547
Tremaine, S., et al. 2002, ApJ, 574, 740
Umemura, M. 2001, ApJ, 560, L29
Umemura, M., Loeb, A., & Turner, E. L. 1993, ApJ, 419, 459
Veilleux, S., Kim, D.-C., & Sanders, D. B. 2002, ApJS, 143, 315
Veilleux, S., Sanders, D. B., & Kim, D.-C. 1999, ApJ, 522, 139
Wang, T. G., & Lu, Y. J. 2001, A&A, 377, 52
Watanabe, C., Ohta, K., Akiyama, M., & Ueda, Y. 2004, ApJ, 610, 128
Wu, H., Zou, Z. L., Xia, X. Y., & Deng, Z. G. 1998, A&AS, 132, 181
Zheng, X.,Wu, H., Mao, S., Xia, X.-Y., Deng, Z.-G., & Zou, Z.-L. 1999, A&A, 349, 735
Zheng, X. Z., Xia, X. Y., Mao, S., Wu, H., & Deng, Z. G. 2002, AJ, 124, 18